Solving Time-Dependent Slow Moving Interface Problems in Heat Transfer Using the CVBEM

T.V. Hromadka II and C.C. Yen

Williamson and Schmid, 17782 Sky Park Boulevard, Irvine, CA 92714, USA

Abstract

The Complex Variable Boundary Element Method or CVBEM provides solutions to two-dimensional potential problems. Especially unique to this method is the approximate boundary which represents the true problem boundary transformed to the spatial configuration where the problem's boundary conditions are satisfied.

In this paper, the approximate boundary technique is extended to the temporal term. The resulting approximate boundary represents a time-stepped sequence of geometries where at each time-step, the problem's boundary conditions are satisfied. This continually deforming approximate boundary indicates a true measure of numerical accuracy which although based on highly sophisticated analytic function theory, is easy to interpret and understand.

Applications of this new technique are demonstrated in studying slow moving interface problems involving the freezing and thawing of two-dimensional domains.

Introduction

For two-dimensional soil freezing problems with slowly moving freezing fronts and homogeneous-isotropic materials, the Complex Variable Boundary Element Method or CVBEM may be used as an approximate model of the prototype system (Hromadka and Guymon, 1984). Additionally, the CVBEM permits a direct and immediate determination of the numerical approximation error in solution of a Laplacian equation system developing the associated approximate boundaries (Hromadka, 1984a). Thus the numerical solution error can be evaluated by observing the deviation of the approximate boundary from the true problem boundary, and the deviation between the approximate boundaries in the location of the freezing front contour which divides the problem domain into a frozen and thawed region (Hromadka, 1986). Thus, the modeling accuracy is evaluated by the model-user in the determination of an approximate boundary upon which the CVBEM provides an exact solution. Although nonhomogeneity (and anisotropy) can be included in the CVBEM model, the resulting fully populated matrix system quickly becomes large. Therefore in this development, the domain is assumed homogeneous and isotropic except

for differences in frozen and thawed conduction parameters on either side of the freezing front. It is noted that although this section is focused upon the prediction of steady state interface conditions for soil freezing problems, the technique is directly applicable to other slow-moving interface problems where potential theory, applied for quasi steady-state conditions, develop flux values of the state variable to within a reasonable accuracy to the true time-stepped solution.

Modeling Approach

The modeling approach (the governing equations and modeling assumptions are given in Hromadka, 1984b) initiates by developing a CVBEM approximator $\hat{\omega}_f(z)$ and $\hat{\omega}_t(z)$ for the frozen and thawed domains, respectively. The numerical technique determines the analytic function $\hat{\omega}(z)$ which satisfies the boundary conditions of either normal flux or temperature specified at nodal points located on the problem boundary, Γ. Because $\omega(z)$ is analytic throughout the interior domain Ω which is enclosed by Γ, then the real and imaginary parts of $\hat{\phi}(z) + i\,\hat{\psi}(z)$ both exactly satisfy the Laplace equation over Ω. (As discussed previously, this property afforded by the CVBEM is not guaranteed by any of the domain methods such as finite elements or finite differences.)

For the steady state condition, the governing heat flow equations reduce to the Laplace equations. Consequently, an $\hat{\omega}(z)$ determined for both the frozen and thawed regions satisfy the Laplace equations exactly, leaving only errors in satisfying the boundary conditions. To develop a CVBEM steady state solution, an $\hat{\omega}(z)$ is developed for each of the separate regions. Initially, both $\hat{\omega}_f(z)$ and $\hat{\omega}_t(z)$ are defined by

$$\hat{\omega}_f(z) = \hat{\omega}_f^1, \quad z \in \Omega$$
$$\hat{\omega}_t(z) = \hat{\omega}_t^1, \quad z \in \Omega \qquad (1)$$

where $\Omega = \Omega_t \cup \Omega_f$ is the global domain, and the first order CVBEM approximators are based on the entire domain. This procedure results in simply estimating the 0°C isotherm location for the homogeneous problem of Ω being entirely frozen or thawed. Let C^1 be the contour corresponding to this 0°C isotherm.

The second iteration step begins by defining Ω_f^2 and Ω_t^2 based on the mutual boundary of C^1. CVBEM approximators $\hat{\omega}_f^2$ and $\hat{\omega}_t^2$ are then defined for Ω_f^2 and Ω_t^2, respectively (e.g. Hromadka, 1986).

Examining the stream functions $\hat{\psi}_f^2$ and $\hat{\psi}_t^2$, estimates of the discrepancy in matching the flux rates along the interface between Ω_t and Ω_f can be evaluated. The $\hat{\omega}_f^2$ function is now used to determine the next location of the 0°C isotherm. This is accomplished by determining a new $\hat{\omega}_f^*$ with the stream function values of $\hat{\omega}_t^2$ (and modified by conductivity) superimposed at the nodal values of C^1. Next, a new 0°C isotherm C^* is located for $\hat{\omega}_f^*$. The next estimated location for the 0°C isotherm, C^2, is located by averaging the y-coordinates of the nodal points between C^1 and C^*. Figure 1 illustrates this procedure.

where Γ is a simple closed contour enclosing a simply connected domain Ω; ζ is the variable of integration with $\zeta \in \Gamma$; z is a point in Ω; and the direction of integration is in the usual counterclockwise (positive) sense (fig. 1). The function $G(\zeta)$ is a global trial function which is continuous on Γ. The linear global trial function is defined by

$$G(\zeta) = \sum_{j=1}^{m} \delta_j (N_j \bar{\omega}_j + N_{j+1} \bar{\omega}_{j+1}) \tag{7}$$

where $\delta_j = 1$ if $\zeta \in \Gamma_j$, and $\delta_j = 0$ if $\zeta \notin \Gamma_j$. In this case, the functions N_j and N_{j+1} are the usual linear basis functions. From the definition of $G(\zeta)$ we have

$$\int_{\Gamma} \frac{G(\zeta)d\zeta}{\zeta - z} = \int_{U\Gamma_j} \frac{G(\zeta)d\zeta}{\zeta - z} = \sum_{j=1}^{m} \int_{\Gamma_j} \frac{G(\zeta)d\zeta}{\zeta - z} = \sum_{j=1}^{m} \int_{\Gamma_j} \frac{(N_j \bar{\omega}_j + N_{j+1}\bar{\omega}_{j+1})d\zeta}{\zeta - z} \tag{8}$$

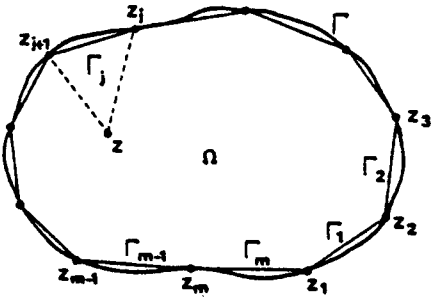

Fig. 1. CVBEM Boundary Discretization

Γ_j = Boundary element linking nodes j and j+1;

z_j = Nodal coordinate for node j, ($z_{m+1} = z_1$);

Γ = Natural boundary

The CVBEM continues by using (8) to develop m equations as a function of the m unknowns associated with the undetermined nodal values of either $\bar{\phi}$ or $\bar{\psi}$ at each node. That is, $\bar{\omega} = \bar{\phi} + i\bar{\psi}$ where $\bar{\phi}$ and $\bar{\psi}$ are nodal values of the potential and stream functions respectively. Given m nodes specified on Γ_j, we necessarily know either $\bar{\phi}$ or $\bar{\psi}$ (not both) at each z_j, $j = 1,2,\cdots,m$. Then to estimate the remaining m nodal values, $\hat{\omega}(z)$ is collocated in the form of a Fredholm equation by forcing

$$\text{CLASS I:} \qquad \bar{\phi}_k(z_j) = \text{Re}\ \hat{\omega}(z_j) \qquad \bar{\psi}_k(z_j) = \text{Im}\ \hat{\omega}(z_j) \tag{9a}$$

$$\text{CLASS II:} \qquad \bar{\phi}_u(z_j) = \text{Re}\ \hat{\omega}(z_j) \qquad \bar{\psi}_j(z_j) = \text{Im}\ \hat{\omega}(z_j) \tag{9b}$$

In the above, the subscript u and k refer to unknown and known boundary condition nodal values, respectively. Because $\hat{\omega}(z_j) = \hat{\omega}(\bar{\phi}_k, \bar{\phi}_u, \bar{\psi}_k, \bar{\psi}_u)$, then a $\hat{\omega}(z)$ is determined by either (9a) or (9b) for $j = 1, 2, \cdots, m$. The difference between these two approximations is that the Class I system results in a CVBEM approximator which matches all the known nodal-point boundary-condition values, whereas the Class II system results in an approximation which equals the CVBEM-estimated unknown nodal-point boundary-condition values.

Nodal equations are determined by taking the limit as the point $z \in \Omega$ approaches a selected nodal point $z_j \in \Gamma$ by

$$\hat{\omega}(z_j) = \lim_{z \to z_j^-} \frac{1}{2\pi i} \int_\Gamma \frac{G(\zeta)\, d\zeta}{\zeta - z} \tag{10}$$

The limiting value is also known as the Cauchy principal value, and by using either the Class I or Class II systems, a set of m equations results; these equations are solvable for the unknown nodal values by the usual matrix-solution techniques such as Gaussian elimination.

Flow Field Model

Due to the linearity of Laplace's equation, one can superimpose as many flow components as required to obtain the general expression for the complex velocity potential of the entire system. A potential function F(z) which described one or several point sources of contaminant recharge, together with some groundwater discharging wells, combined with a uniform regional groundwater flow regime, is developed that exactly satisfies the Laplace equation in domain Ω by

$$F(z) = \hat{\omega}(z) + \sum_{i=1}^{n} \frac{Q_i}{2\pi T} \text{Ln}\ (z - z_i), \quad z \in \Omega \tag{11}$$

where Q_i is the discharge from well i (of n) located at z_i [i.e. (+) for a sink; (-) for a source], T is the transmissivity of a confined aquifer, and $\hat{\omega}(z)$ is a CVBEM approximator representing the background flow field. In Eq. (11), F(z) must satisfy the boundary conditions

$$\xi(z) = \delta\phi(z) + i(1 - \delta)\ \psi(z), \quad z \in \Gamma \tag{12}$$

where $\delta = 1$ if $\phi(z)$ is known; $\delta = 0$ if $\psi(z)$ is known; and $\xi(z)$ is a boundary-condition distribution along Γ.

The source and sink terms included in Eq. (11) represent an exact model for steady state flow. Thus, $\xi(z)$ must be modified in order to develop a CVBEM $\hat{\omega}(z)$ by

$$\xi^*(z) = \xi(z) - \sum_{j=1}^{n} \frac{Q_i}{2\pi T} \text{Ln } (z - z_i), \quad z \in \Gamma \tag{13}$$

The flow field is then determined by collocating $\hat{\omega}(z)$ at each node $z_j \in \Gamma$ according to the boundary-condition distribution of $\xi^*(z)$. The resulting analytic function $F(z)$ describes the CVBEM model. In Eq. (13), $\xi^*(z)$ is defined according to the real and imaginary parts as given in Eq. (12).

Poisson Equation

Given a continuous distribution of sources (such as from precipitation) in a flow field in domain Ω, the steady state flow model must be extended to accommodate the Poisson equation, with k as a constant,

$$\frac{\partial^2 \phi}{\partial x^2} + \frac{\partial^2 \phi}{\partial y^2} = k \tag{14}$$

Equation (14) can be modeled by choosing a particular solution ϕ_p such that

$$\frac{\partial^2 \phi_p}{\partial x^2} + \frac{\partial^2 \phi_p}{\partial y^2} = k \tag{15}$$

For example, $\phi_p = \frac{k}{4}(x^2 + y^2)$ is a suitable choice (an infinity of other particular solutions are available). After choosing ϕ_p, the boundary condition function $\xi(z)$ is modified in order to develop $\hat{\omega}(z)$ by

$$\xi^*(z) = \xi(z) - \sum_{i=1}^{n} \frac{Q_i}{2\pi T} \text{Ln } (z - z_i) - \phi_p(z), \quad z \in \Gamma \tag{16}$$

The CVBEM approximator $\hat{\omega}(z)$ is collocated at nodes z_j with respect to the $\xi^*(z)$ function. Thus, the Poisson equation is exactly solved by

$$F(z) = \hat{\omega}(z) + \sum_{i=1}^{n} \frac{Q_i}{2\pi T} \text{Ln } (z - z_i) + \phi_p(z) \tag{17}$$

The above procedure can be extended to the relation

$$\frac{\partial^2 \phi}{\partial x^2} + \frac{\partial^2 \phi}{\partial y^2} = f(x,y) \tag{18}$$

by choosing a ϕ_p such that Eq. (18) is satisfied, and proceeding with the development of an appropriate CVBEM $\hat{\omega}(z)$ in the same way.

Solute Transport Model

The solute transport mechanism is assumed only applicable to the modeling of steady state, advective contaminants, for those which move with the groundwater flow. The solute-transport process is approximated by calculating point-flow velocities given by the derivative of the potential function $\phi(z)$ where

$$\phi(z) = \text{Re } F(z) \tag{19}$$

The extent or boundary of the subsurface contamination is then evaluated according to point values of the flow velocity and the time increment selected. Point flow velocities are estimated as

$$u = -K \frac{\partial \phi}{\partial x} / \theta_0 \tag{20a}$$

$$v = -K \frac{\partial \phi}{\partial y} / \theta_0 \tag{20b}$$

where (u,v) are (x,y)-direction soil-water flow velocities, K is the saturated hydraulic conductivity, and θ_0 is the effective porosity of the aquifer material. (A retardation factor, r, can be included in the denominator of Eq. (20) in order to account for contaminant transport velocities being less than the actual field velocity or specific discharge.)

The velocity of a contaminant particle is used to estimate the distance traveled along a flow field streamline by the approximations

$$\frac{dx^*}{dt} = u \tag{21a}$$

$$\frac{dy^*}{dt} = v \tag{21b}$$

where in the above (x^*, y^*) are the coordinates of the subject contaminant particle.

Applications

Application 1

Figure 2 shows a completely penetrating groundwater well (discharge 50 m^3/hr) located at the coordinates (300, 300) in a homogeneous isotropic aquifer of thickness 10 m. Contaminated water is being recharged (recharge of 50 m^3/hr) at a second well (injection well) located at the coordinates (300, -300) with a distance of 848.5 m from the supply well (discharge well). Effective porosity is 0.25, saturated hydraulic conductivity is 1 m/hr, and negligible background groundwater flow is assumed. Retardation is assumed to be 1.

Depicted in Fig. 2 are the limits of groundwater contamination corresponding to model times of 0.5, 2, and 4 years. Additionally, the CVBEM model predicts a first arrival of contamination of time 4.33 years for injected water to reach the pumping site which agrees well with the Javendal et al. [1985] estimate of 4.3 years.

Application 2

Two discharge wells are added at the coordinates (+500, +500) in application 1. Figure 3 depicts the contaminant front at 0.5, 2, and 4 years. It takes 4.32 years for the contaminant water to reach the middle discharge well (-300, 300), and about 5.58 years for the contaminant water to reach the other two production wells.

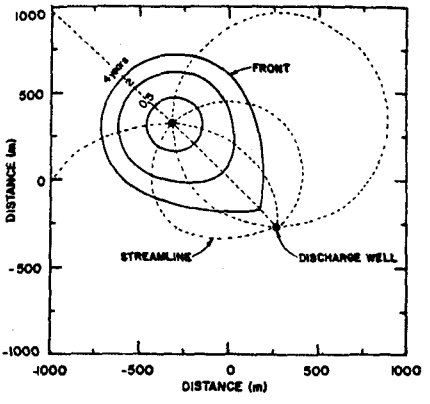

Fig. 2. Flowline pattern and front positions between injection and production well for application 1

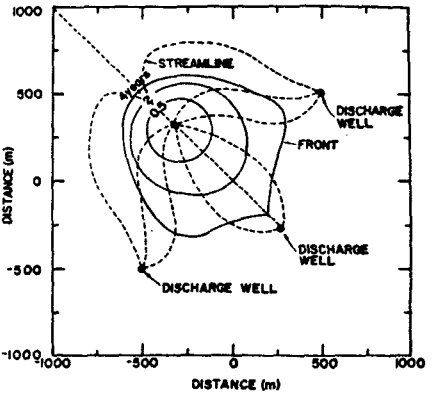

Fig. 3. Flowline pattern and front positions between injection and three production wells for application 3

Application 3

Let's consider the steady flow pattern produced by a single pumping well whose strength equals to 50 m^3/hr at (0,0) near a landfill site with an equipotential boundary ϕ = 2 m along y = - 1000. It took the contaminant front 8.96 years to reach the pumping well. Two additional injection wells were installed at (-500, 250) and (-500, -250) with strength equal to 10 m^3/hr, to retard the contaminant front. Figures 4 and 5 depict the front movements of these two case problems.

Application 4

In this problem, a liquid-waste disposal pond with a diameter of 100 m fully penetrates the aquifer is added to application 3. The center of this pond has coordinates of (500, 500) on the Cartesian system shown in Fig. 6. Liquid level in the pond is such that the volume rate of leachate leaving the pond is about 20 m^3/hr. It takes 15.7 years and 7.3 years for the contaminant liquid to reach the discharge well from the left boundary and from the disposal pond, respectively.

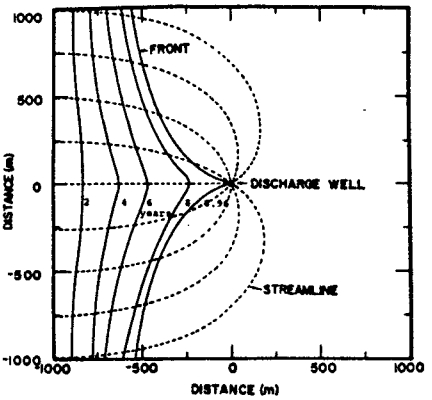

Fig. 4. Flowline pattern and front positions between equipotential boundary and discharge well

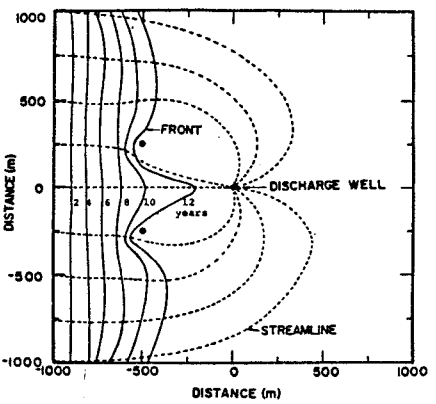

Fig. 5. Flowline pattern and front positions between two retarding wells and production well for application 3

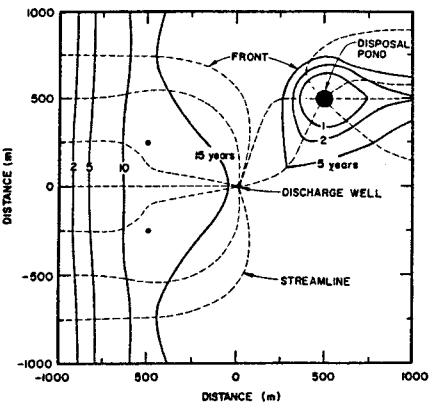

Fig. 6. Flowline pattern and front positions for application 4

Summary and Conclusions

In this paper, the CVBEM is used to develop a model of steady-state, advective, contaminant transport in ground-water. Because with the CVBEM approach the Laplace and Poisson partial differential equations are solved exactly, all modeling error occurs in matching the prescribed boundary conditions.

The presented model considers steady-state conditions for two-dimensional ground-water flows. The modeling technique is not applicable to three-dimensional problems. However, the modeling approach can be extended to include various steady-state boundary conditions, regional nonhomogeneity and anisotropy.

Because the modeling technique is based upon a boundary integral equation approach, domain mesh generators or control-volume (finite element) discretizations are not required. Nodal points are required only along the problem boundary rather than in the interior of the domain. Consequently, the computer-coding

requirements are small and can be accommodated by many currently available home computers.

References

1. Hromadka II, T. V., Linking the Complex Variable Boundary Element Method to the Analytic Function Method, Numerical Heat Transfer, Vol. 7, No. 2, (1984a), pg. 235-240.

2. Hromadka II, T. V., The Complex Variable Boundary Element Method, Springer-Verlag, (1984b), 250 pgs.

3. Javendal, I., Doughty, C., and Tsang, C. F., A Handbook for the Use of Mathematical Models for Subsurface Contaminant Transport Assessment, AGU Monograph, (1985).